Peer-reviewed version available at Polymers 2019, 11, 375; doi:10.3390/polym11020375

Type of the Paper (Article)

Facile Synthesis of Methylsilsesquioxane Aerogels with Uniform Mesopores by Microwave Drying

Xingzhong Guo [1,*], Jiaqi Shan [1], Wei Lei [2], Ronghua Ding [2], Yun Zhang [2] and Hui Yang [1]

[1] School of Materials Science and Engineering, Zhejiang University, Hangzhou 310027, China; 21626008@zju.edu.cn (J.S.); yanghui@zju.edu.cn (H.Y.)
[2] Pan Asia Microvent Tech (Jiangsu) Coporation & Zhejiang University Micro-nano-porous Materials Joint Research Development Center, Changzhou 213100, China; leiwei@microwent.com.cn (W.L.); dingronghua@microvent.com.cn (R.D.); zhangyun@microvent.com.cn (Y.Z.)
* Correspondence: msewj01@zju.edu.cn; Tel.: +86-571-8795-3313

Abstract: Methylsilsesquioxane aerogels with uniform mesopores have been facilely prepared via a sol–gel process followed by microwave drying with methyltrimethoxysilane (MTMS) as precursor, hydrochloric acid (HCl) as catalyst, water and methanol as solvents, hexadecyltrimethylammonium chloride (CTAC) as surfactant and template and propylene oxide (PO) as gelation agent. The microstructure, chemical composition and pore structures of the resultant MSQ aerogels were investigated in detail to achieve controllable preparation of MSQ aerogels, and the thermal stability of MSQ aerogels was also analyzed. The gelation agent, catalyst, solvent and microwave power have important roles on pore structures of MSQ aerogels. Meanwhile, microwave drying method is found to not only have a remarkable effect on improving production efficiency, but also be conducive to avoid the collapse of pore structure especially micropores during drying. The resulting MSQ aerogel microwave-dried at 500 W possesses a specific surface area up to 821 m^2/g and a mesopore size of 20 nm, and displays good thermal stability.

Keywords: MSQ aerogel; mesoporous structure; sol-gel; microwave drying

1. Introduction

Silica aerogel is a low-density porous solid material with three-dimensional reticulate skeletons formed by interconnected SiO_2 nanoparticles [1]. Benefited from its special structure, silica aerogel possesses various unique properties [2-5] such as high specific surface area and porosity, low thermal conductivity, high visible-light transmittance and low dielectric constant. Owing to these properties, silica aerogel has been applied in various fields such as catalyst carrier [6-8], heat insulation [9-11], acoustic insulation [12-14], Cherenkov radiation detectors [15] and adsorbent [16-19], thermal energy storage [20]. Silica aerogel was first prepared by S. S. Kistler in 1930s via supercritical drying [21]. Until now, supercritical drying is still an effective method to avoid aerogel's shrinkage and cracks during drying. However, supercritical drying, which needs special conditions such as high pressure and high temperature, prevents aerogels from industrial manufacturing and extended applications. Therefore, the preparation of silica aerogel by ambient pressure drying becomes a hot research topic in these years. One practical way is to use organoalkoxysilanes with small organic substituent groups to obtain organic-inorganic hybrid aerogel. Methylsilsesquioxane (MSQ) aerogel [22-24] is a methyl hybrid silica aerogel, derived from organoalkoxysilanes with methyl groups through a facile sol-gel process [25,26]. Methyl group was introduced in order to enhance mechanical strength of aerogel's skeletons formed by interconnected nanoparticles, which has been proved to be effective.

Therefore, in the last few years, lots of research efforts were devoted to the synthesis of silica aerogels by ambient pressure drying. Song He et al. [27] reported the experimental results on the synthesis of water glass based silica aerogels dried under ambient pressure, using N, N-dimethylformamide (DMF) as drying control chemical additive (DCCA), trimethylchlorosilane (TMCS) for surface modification, ethanol and n-hexane for solvent replacement, in which DCCA and

TMCS used to reduce the capillary during drying were environment-unfriendly and poisonous preventing aerogels from extended applications. To avoid using DCCA and surface modifier, Gen Hayase et al. [28] reported the preparation of transparent MSQ aerogels via a facile sol-gel process, using methanol, 2-propanol and heptane for multistage solvent replacement, in which a kind of "aging sol" was used to enhance mechanical strength of aerogel's skeleton for reducing the capillary during drying. This preparation method was environment-friendly but not efficient which took extra 3 days for preparation of aging sol, soak of aging sol and evaporation at room temperature preventing MSQ aerogels from industrial manufacturing.

In this study, methylsilsesquioxane (MSQ) aerogels have been easily prepared by a sol–gel process using methyltrimethoxysilane (MTMS) as precursor, hydrochloric acid (HCl) as catalyst, water and methanol as solvents, hexadecyltrimethylammonium chloride (CTAC) as surfactant and template and propylene oxide (PO) as gelation agent [25,26,29], methanol, 2-propanol and heptane for multistage solvent replacement, followed by microwave drying. The pH, solvent polarity and volume and microwave power have important roles on the pore structures of MSQ aerogels, and the controllable preparation of MSQ aerogels with uniform mesopores can be facilely achieved by microwave drying. Meanwhile, we found that microwave drying not only has a remarkable effect on improving production efficiency, but also is conducive to avoid collapse of pore structure especially micropores resulted from thermal gradients during drying.

2. Results and discussion

2.1. Controllable preparation of MSQ aerogels with uniform mesopores

2.1.1. Effect of gelation agent (PO) on pore structures of MSQ aerogels

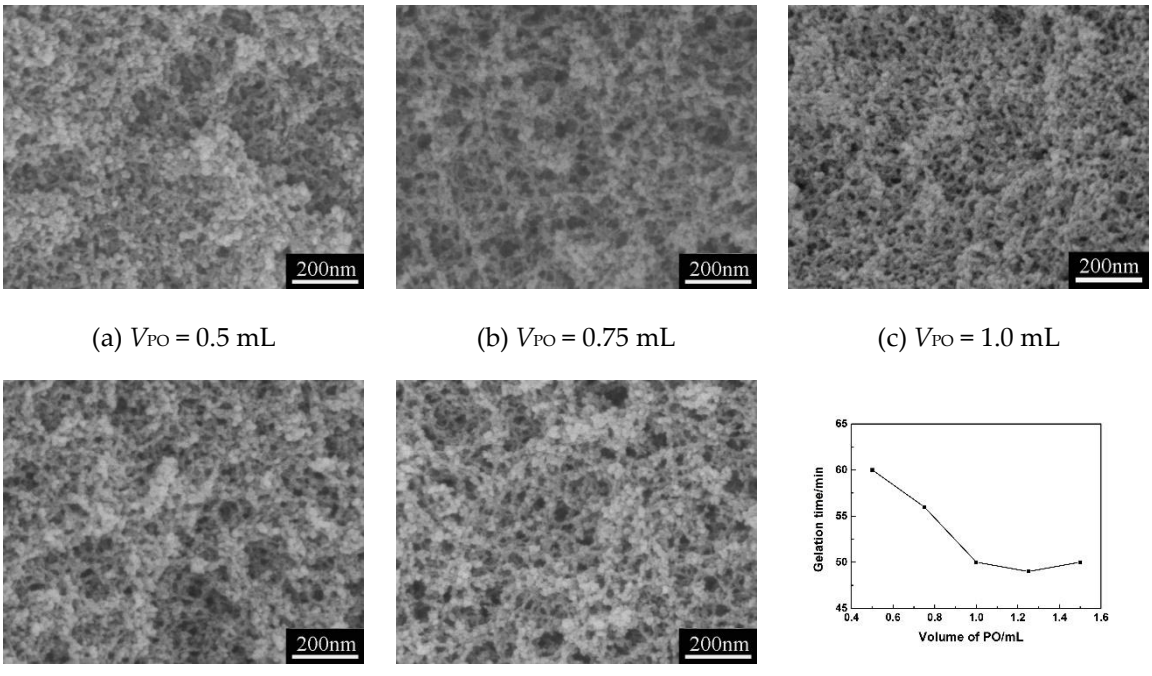

(a) V_{PO} = 0.5 mL (b) V_{PO} = 0.75 mL (c) V_{PO} = 1.0 mL

(d) V_{PO} = 1.25 mL (e) V_{PO} = 1.5 mL (f) Relationship between gelation time and PO volume

Figure 1. SEM images (a~e) of MSQ aerogels prepared by 350 W microwave drying via varied sol-gel processes with different PO volumes (V_{PO}) and (f) gelation time (t) of MSQ aerogels prepared by 350 W microwave drying via varied sol-gel processes with different solvent volumes (V_{PO}).

Figures 1a~1e show SEM images of MSQ aerogels prepared via varied sol gel processes with different volumes of gelation agent (PO), and Figure 2f shows gelation time (t) of MSQ aerogels prepared with different volumes of PO. With the increase of PO volume, the gelation time of aerogels

decreases until the volume of PO is 1.0 mL, which indicates that 1.0 mL of PO is enough to participate in ring opening reaction with HCl for slowly elevating pH of sol. However, when the volume of PO increases from 1.0 to 1.5 mL, the mesopores of aerogels become larger, the reason of which is that the extra part of PO indirectly increases the volume of liquid phase. Similarly, it can be used to explain the change of microstructure of aerogels from Figures 1a to 1b. However, with the increase of PO volume, the gelation time of aerogels has a marked decline, which leads to inadequate separation of solid and liquid phases. As a result, we conclude that 1.0 mL of PO is appropriate in the sol-gel preparation of MSQ aerogels.

2.1.2. Effect of catalyst (HCl) on pore structures of MSQ aerogels

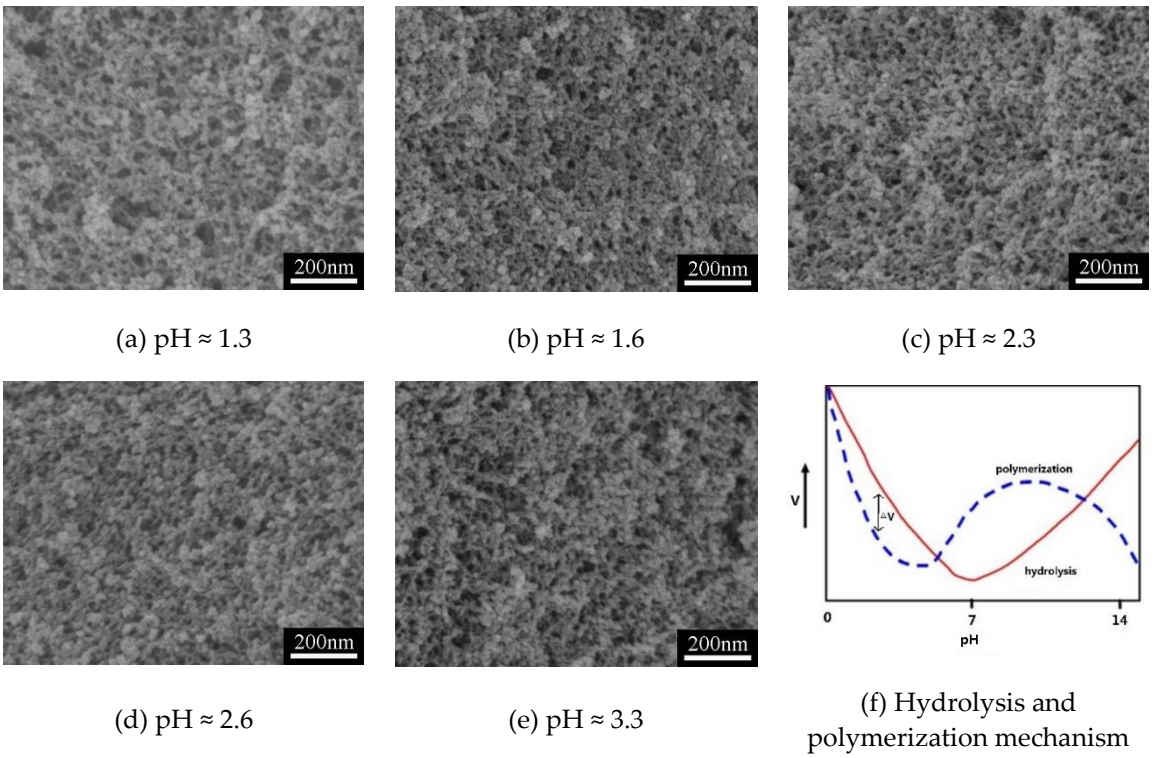

(a) pH ≈ 1.3 (b) pH ≈ 1.6 (c) pH ≈ 2.3

(d) pH ≈ 2.6 (e) pH ≈ 3.3 (f) Hydrolysis and polymerization mechanism

Figure 2. SEM images (a~e) of MSQ aerogels prepared by 350 W microwave drying via varied sol-gel processes with different pH conditions and hydrolysis and polymerization mechanism of MSQ aerogel (f) [30].

Figures 2a~2e show SEM images of MSQ aerogels prepared via varied sol-gel processes with different concentrations of HCl solutions, and Figure 4f shows variation of the velocity of hydrolysis and polymerization with pH [30]. According to the mechanism of hydrolysis and polymerization reactions of MTMS, the smaller the difference between velocity of hydrolysis and polymerization (ΔV) is, the smaller the nanoparticles of aerogel are. In other words, there must be a point of pH with which the nanoparticles of aerogel prepared to be smallest. However, when the pH value increases from 1.3 to 3.3 in this sol-gel system, the microstructure of MSQ aerogel changes little, the reason of which is that in sol-gel process the hydrolysis and polymerization reactions of MTMS carry out under ice bath condition. Both the velocity of hydrolysis and polymerization is lowly resulted in little change of ΔV. Figure 3 shows N_2 adsorption–desorption isotherms (a) and BJH mesopore size distributions (b) of MSQ aerogels prepared with different pH conditions, and the pore structures of MSQ aerogels are listed in Table 1. As observed from Figure 3 and table 1, with the increase of pH, the isotherms, mesopore size distributions and pore structure data of aerogels also change little, which is corresponding to Figures 2a~2e. In this sol-gel system, the reaction condition of ice bath not only avoids the temperature effect caused by exothermic hydrolysis reaction, but also reduces the effect of catalyst concentration on the structure of MSQ aerogels, which is advantageous to improve the stability of MSQ aerogels production.

Preprints (www.preprints.org) | NOT PEER-REVIEWED | Posted: 15 January 2019 doi:10.20944/preprints201901.0147.v1

Peer-reviewed version available at Polymers 2019, 11, 375; doi:10.3390/polym11020375

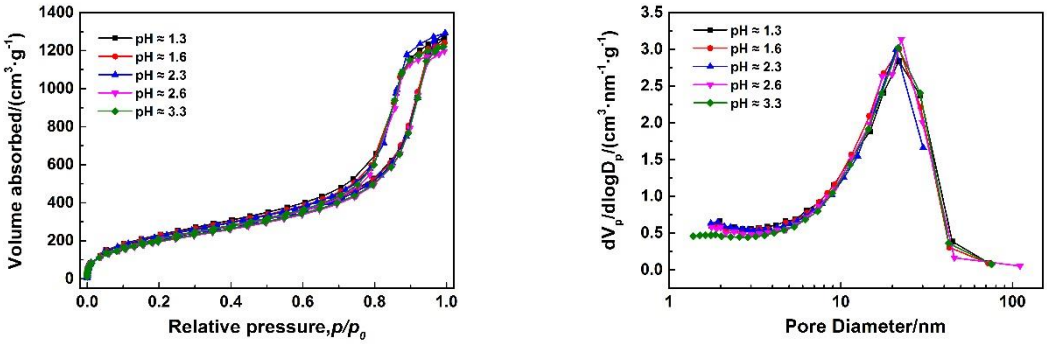

(a) N_2 adsorption–desorption isotherms (b) BJH mesopore size distributions

Figure 3. N_2 adsorption–desorption isotherms (a) and BJH mesopore size distributions (b) of MSQ aerogels prepared by 350 W microwave drying via varied sol-gel processes with different pH conditions.

Table 1. Pore structure data of MSQ aerogels prepared 350 W microwave drying via varied sol-gel processes with different pH conditions.

pH	S_p[a] (m^2/g)	V_{pore}[b] (cc/g)	S_{micro}[c] (m^2/g)	V_{micro}[c] (cc/g)
1.3	786	1.9	588	0.3
1.6	789	1.9	580	0.3
2.3	784	1.9	596	0.3
2.6	731	1.8	547	0.3
3.3	759	1.8	552	0.3

[a] Brunauer–Emmett–Teller specific surface area. [b] Pore volume calculated by NLDFT method from the adsorption branch. [c] Micropore surface and volume calculated by the Dubinin-Astakhov method.

2.1.3. Effect of solvent on pore structures of MSQ aerogels

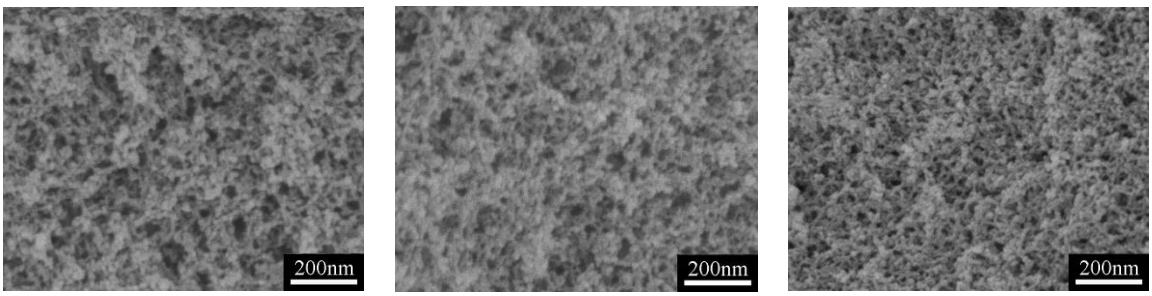

(a) $M/W \approx 0.33$ (b) $M/W = 0.5$ (c) $M/W = 1.0$

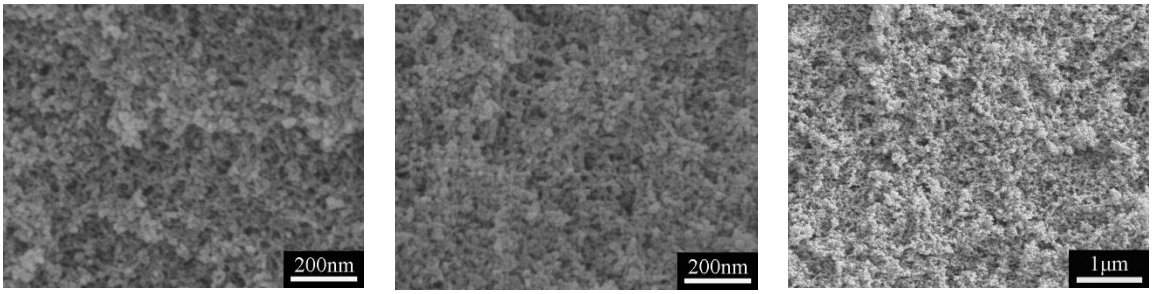

(d) $M/W = 2.0$ (e) $M/W = 3.0$ (f) $M/W = 0$

Figure 4. SEM images of MSQ aerogels prepared by 350 W microwave drying via varied sol-gel processes with different solvent polarity. (Solvent polarity was adjusted by changing volume ratios of methanol (*M*) and water (*W*), *M*/*W*)

Figures 4a~4f show SEM images of MSQ aerogels prepared by 350 W microwave drying via varied sol-gel processes with different solvent polarity. Compared Figure 4a with 4f, it is found that without addition of methanol, the microstructure of MSQ aerogel becomes more compact because in this sol-gel process methanol is an indispensable solvent not only to dissolve and disperse MTMS and CTAC but also to restrain the hydrolysis and condensation of MTMS. With the increase of the volume ratios of methanol and water (*M*/*W*), the sizes of mesopores and nanoparticles of resultant MSQ aerogels successively become smaller because of successively decreasing phase separation in their sol-gel processes. According to Flory Huggins lattice theory [31], in two phase mixed system, the larger the polarity difference between two phases become, the larger the phase separation trend is. So with the increase of *M*/*W*, the polarity difference between component solvent and sol derived from MTMS becomes small, indicating a low phase separation. Therefore, we conclude that it is effective to achieve controllable preparation of MSQ aerogels by adjusting polarity of component solvent. Figures 5a~5e show TEM images of MSQ aerogels prepared with different solvent polarity, and Figure 5f shows diagram of phase separation [32]. The change regulation of Figures 5a~5e are in accord with the process of phase separation in Figure 5f, which further demonstrates that the solvent polarity determines the degree of phase separation in this sol-gel system, which is reliable for controllable preparation of MSQ aerogels. Figure 6 shows N_2 adsorption–desorption isotherms (a) and BJH mesopore size distributions (b) of MSQ aerogels prepared by 350 W microwave drying via varied sol-gel processes with different solvent polarity. As the increasing of *M*/*W* from 0.33 to 3.0, the value of volume absorbes and pore diameter gradually decreases, resulting from increasing trend of phase separation between component solvent and skeletons, which is consistent with microstructure characterization above (Figure 4). Table 2 shows pore structures of MSQ aerogels prepared 350 W microwave drying via varied sol-gel processes with different solvent polarity. The specific surface area of MSQ aerogel without methanol is far less than those of MSQ aerogels with methanol, which is also consistent with microstructure characterization above.

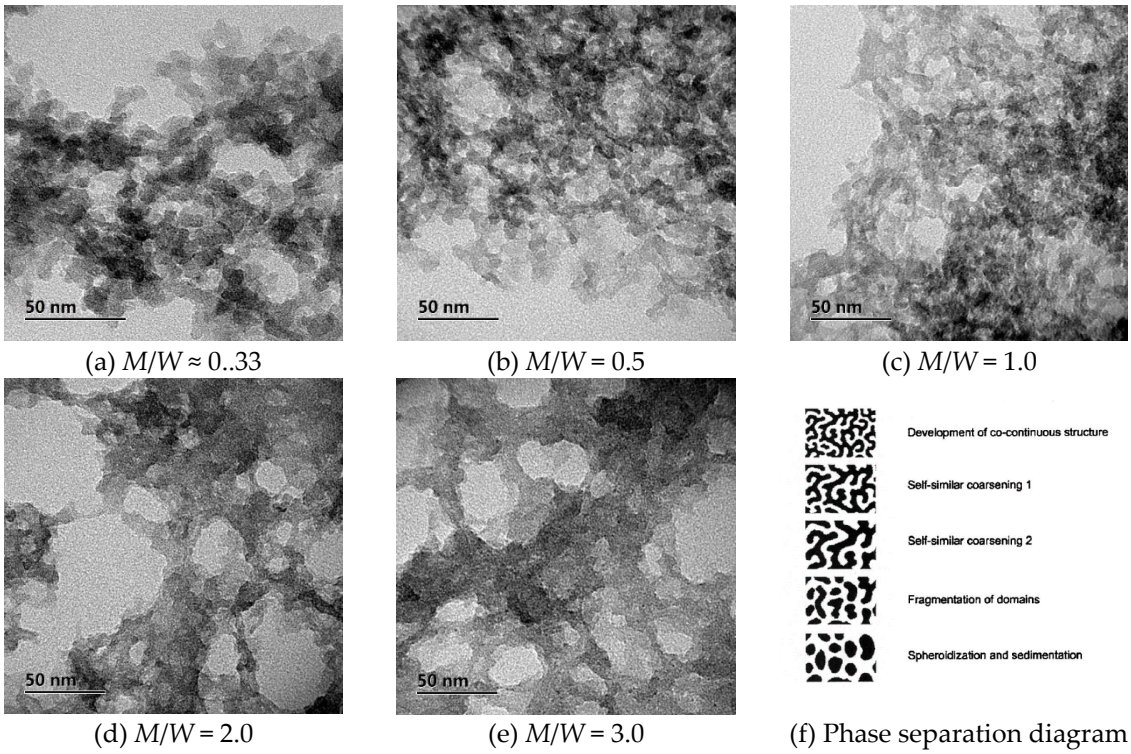

(a) *M*/*W* ≈ 0..33 (b) *M*/*W* = 0.5 (c) *M*/*W* = 1.0

(d) *M*/*W* = 2.0 (e) *M*/*W* = 3.0 (f) Phase separation diagram

Preprints (www.preprints.org) | NOT PEER-REVIEWED | Posted: 15 January 2019 doi:10.20944/preprints201901.0147.v1

Peer-reviewed version available at Polymers 2019, 11, 375; doi:10.3390/polym11020375

Figure 5. TEM images (a~e) of MSQ aerogels prepared by 350 W microwave drying via varied sol-gel processes with different solvent polarity. (Solvent polarity was adjusted by changing volume ratios of methanol and water, M/W) and diagram of phase separation (f) [32].

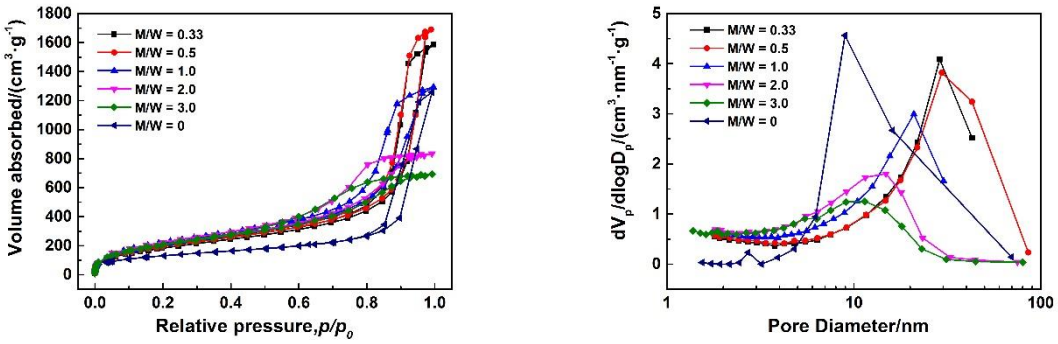

(a) N_2 adsorption–desorption isotherms (b) BJH mesopore size distributions

Figure 6. N_2 adsorption–desorption isotherms (a) and BJH mesopore size distributions (b) of MSQ aerogels prepared by 350 W microwave drying via varied sol-gel processes with different solvent polarity. (Solvent polarity was adjusted by changing volume ratios of methanol and water, M/W)

Table 2. Pore structure data of MSQ aerogels prepared 350W microwave drying via varied sol-gel processes with different solvent polarity. (Solvent polarity was adjusted by changing volume ratios of methanol and water, M/W)

M/W	S_p[a] (m^2/g)	V_{pore}[b] (cc/g)	S_{micro}[c] (m^2/g)	V_{micro}[c] (cc/g)
0.33	702	2.4	494	0.2
0.5	741	2.6	538	0.2
1.0	783	1.9	596	0.3
2.0	782	1.2	575	0.3
3.0	772	1.0	567	0.3
0	472	1.9	52	0.04

[a] Brunauer–Emmett–Teller specific surface area. [b] Pore volume calculated by NLDFT method from the adsorption branch. [c] Micropore surface and volume calculated by the Dubinin-Astakhov method.

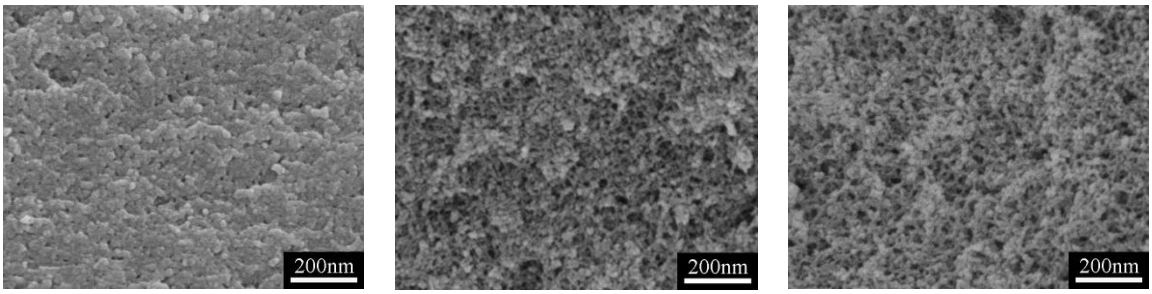

(a) $V \approx 1$ mL (b) $V = 2$ mL (c) $V = 3$ mL

Preprints (www.preprints.org) | NOT PEER-REVIEWED | Posted: 15 January 2019 doi:10.20944/preprints201901.0147.v1

Peer-reviewed version available at Polymers 2019, 11, 375; doi:10.3390/polym11020375

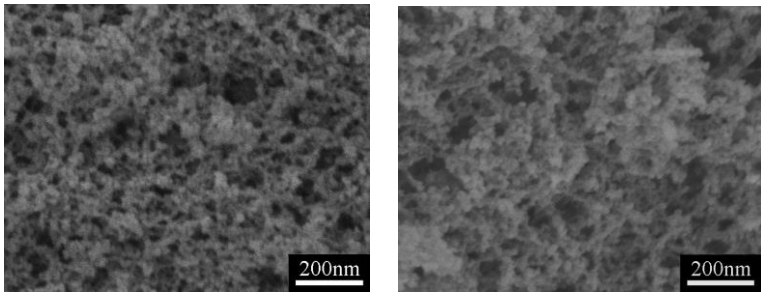

(d) V = 4 mL (e) V = 5 mL

Figure 7. SEM images of MSQ aerogels prepared by 350 W microwave drying via varied sol-gel processes with different solvent volume (V).

Figures 7a~7e show SEM images of MSQ aerogels prepared by 350 W microwave drying via varied sol-gel processes with different solvent volumes. As we known, the pores of aerogels are resulted from the evaporation of solvent. Logically, with the increase of solvent volume, the pore size of MSQ aerogels becomes larger corresponding to figures 7b~7e. However the microstructure of MSQ (a) is too compact whose specific surface area and micropore surface area are much lower than other samples observed from Table 3. It is because in this sol-gel process, 1 mL of solvent is not enough to well dissolve and disperse 3 mL of MTMS and 0.24 g CTAC, leading to the respective agglomeration of sol particles derived from MTMS and micelle derived from CTAC. By adjusting volume of solvent to control the pore size of MSQ aerogels, we can achieve the controllable preparation of MSQ aerogels. Figure 8 shows N_2 adsorption–desorption isotherms (a) and BJH mesopore size distributions (b) of MSQ aerogels prepared by 350 W microwave drying via varied sol-gel processes with different solvent volumes. The isotherm and BJH mesopore size distribution of MSQ aerogel with 1 mL of solvent further confirms its impact microstructure characterized by SEM above. As the solvent volume increases, the pore diameter of MSQ aerogels successively increases, and the pore structure of MSQ aerogels evolves from uniform mesopores to macropores, which is consistent with the result of SEM images in Figure 7.

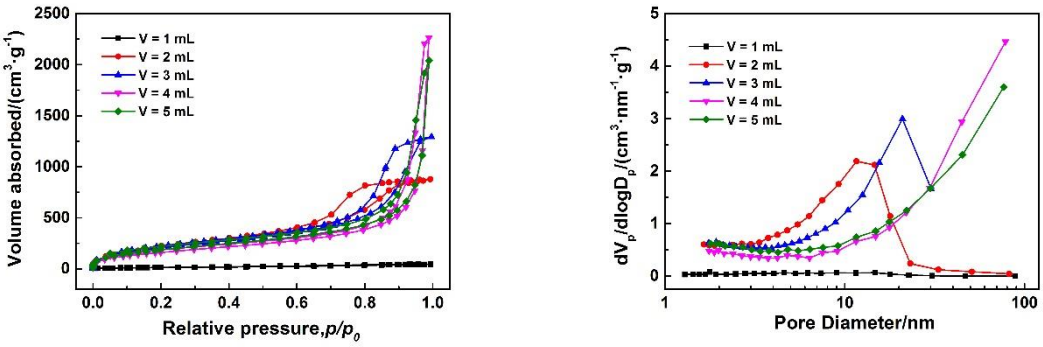

(a) N_2 adsorption–desorption isotherms (b) BJH mesopore size distributions

Figure 8. N_2 adsorption–desorption isotherms (a) and BJH mesopore size distributions (b) of MSQ aerogels prepared by 350W microwave drying via varied sol-gel processes with different solvent volume (V).

Table 3. Pore structure data of MSQ aerogels prepared 350W microwave drying via varied sol-gel processes with different solvent volume (V).

V/mL	S_p[a](m²/g)	V_{pore}[b](cc/g)	S_{micro}[c](m²/g)	V_{micro}[c](cc/g)
1	52	0.06	28	0.01

Preprints (www.preprints.org) | NOT PEER-REVIEWED | Posted: 15 January 2019 doi:10.20944/preprints201901.0147.v1

Peer-reviewed version available at Polymers 2019, 11, 375; doi:10.3390/polym11020375

2	784	1.3	584	0.3
3	784	1.9	596	0.3
4	611	3.3	455	0.2
5	714	3.0	515	0.3

[a] Brunauer–Emmett–Teller specific surface area. [b] Pore volume calculated by NLDFT method from the adsorption branch. [c] Micropore surface and volume calculated by the Dubinin-Astakhov method.

2.1.4. Effect of microwave power on pore structures of MSQ aerogels

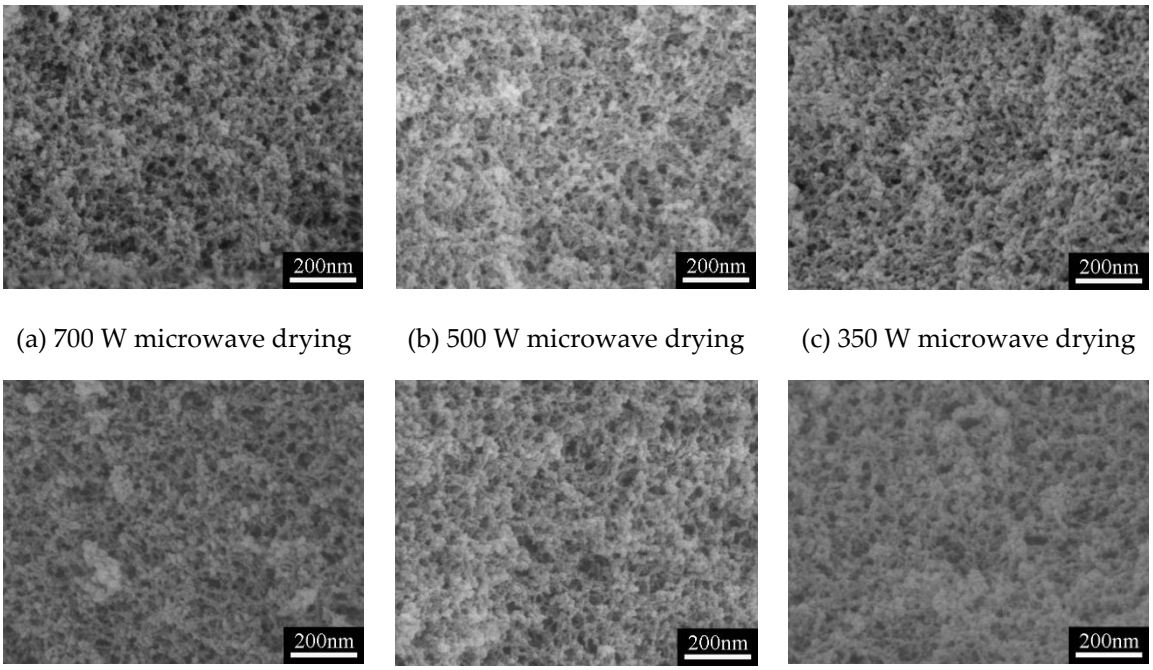

(a) 700 W microwave drying (b) 500 W microwave drying (c) 350 W microwave drying

(d) 200 W microwave drying (e) 40 °C oven drying (f) Indoor evaporation

Figure 9. SEM images of MSQ aerogels prepared by varied microwave power.

To optimize the process of microwave drying and study the influence of microwave power on microstructure of MSQ aerogel, MSQ aerogels prepared by microwave drying at different powers, oven drying and indoor evaporation were characterized by SEM and N_2 adsorption–desorption method. Figures 9a~9d show SEM images of MSQ aerogels prepared by microwave drying at different powers, and Figures 9e and 9f show SEM image of MSQ aerogel prepared by 40 °C oven drying and indoor evaporation respectively. It is observed that the MSQ aerogels prepared by microwave drying has more uniform mesopores than MSQ aerogels prepared by oven drying and evaporation, which benefits from entirety of microwave drying. Also, we conclude that power of microwave has little influence on microstructure of resultant MSQ aerogels in this experiment drying only 10 cm^3 of wet gel. Figure 10(a) shows N_2 adsorption–desorption isotherms of MSQ aerogels prepared by varied drying methods. According to classification of IUPAC, all isotherms of MSQ aerogels prepared by varied drying methods belongs to type IV with a hysteresis loops of type H2, which proves that all the resultant MSQ aerogels have uniform ampuliform mesopores. This shape of mesopores is resulted from skeletons of MSQ aerogel formed by point-connected spherical nanoparticles. Figure 10(b) shows BJH mesopore size distributions of MSQ aerogels prepared by varied drying methods. It is found that the mesopores of MSQ aerogels prepared by 700, 500, 350 W microwave drying mainly distribute at 20 nm while the mesopores of MSQ aerogels prepared by 200 W microwave drying, oven drying and indoor evaporation mainly distributes at 30 nm. As we known, the higher the microwave power is, the faster the rate of microwave heating is. Therefore, we believe that too fast heating rate during microwave drying leads to the irreversible shrinkage of mesopores from 30 to 20 nm. Table 4 shows pore structures of MSQ aerogels prepared by varied drying methods. The specific surface areas of MSQ aerogels prepared by microwave drying are as

high as those prepared by oven drying and evaporation, while the time of microwave drying (less than 1 h) is far less than the time of oven drying (24 h) and evaporation (more than 48 h). Especially, MSQ aerogel prepared by 500 W microwave drying possessed a specific surface area up to 821 m^2/g and a micropore surface up to 617 m^2/g, which proves that the microwave drying is more effective on reducing thermal gradients during drying process than oven drying whose micropore surface is only 491 m^2/g.

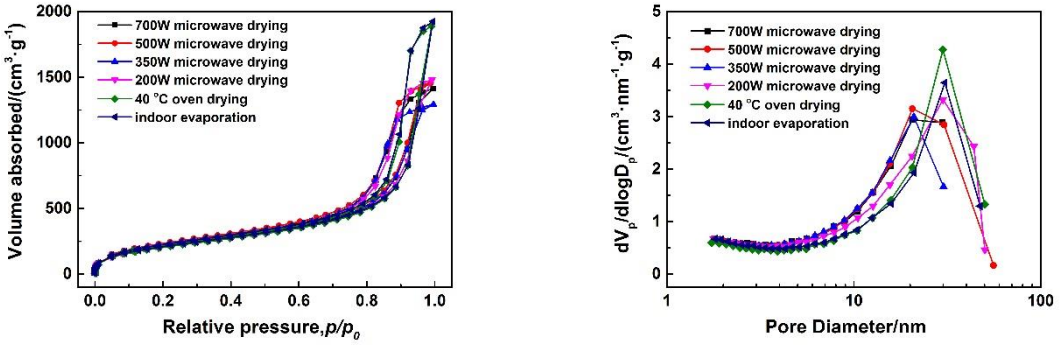

(a) N_2 adsorption–desorption isotherms (b) BJH mesopore size distributions

Figure 10. N_2 adsorption–desorption isotherms (a) and BJH mesopore size distributions (b) of MSQ aerogels prepared by varied drying methods.

Table 4. Pore structure data of MSQ aerogels prepared by varied drying methods.

Drying method	Drying time	S_p[a](m^2/g)	V_{pore}[b](cc/g)	S_{micro}[c](m^2/g)	V_{micro}[c](cc/g)
700W microwave drying	32 min	796	2.1	598	0.3
500W microwave drying	33 min	821	2.2	617	0.3
350W microwave drying	36 min	784	1.9	596	0.3
200W microwave drying	55 min	783	2.1	599	0.2
40 °C oven drying	24 h	714	2.8	491	0.3
indoor evaporation	≥ 48h	795	2.4	610	0.3

[a] Brunauer–Emmett–Teller specific surface area. [b] Pore volume calculated by NLDFT method from the adsorption branch. [c] Micropore surface and volume calculated by the Dubinin-Astakhov method.

2.2. Thermal stability of typical MSQ aerogel

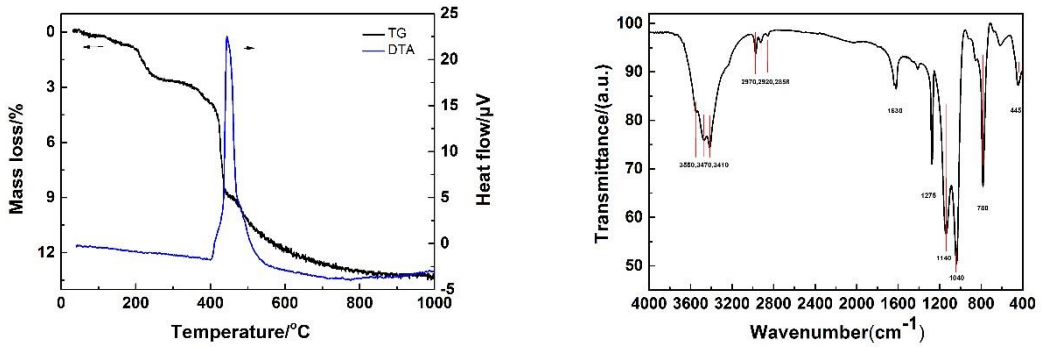

(a) DTA/TG curves (b) IR spectra curve

Figure 11. DTA/TG curves (a) and IR spectrum (b) of a typical MSQ aerogel prepared by microwave drying.

Figure 11(a) shows differential thermal analysis (DTA) and thermogravimetry (TG) curves of a typical MSQ aerogel prepared by microwave drying. When the temperature rises to 200 °C, a mass loss of 3% occurs on TG curve with no peak on DTA curve owing to the slow evaporation of absorbed water. When the temperature rises to 400 °C, methyl groups of MSQ aerogel are oxy-genated, which results in an exothermic peak on DTA curve and mass loss of 6% on TG curve. Without exothermic peak of other reagent, DTA/TG curves prove the high purity of the resultant MSQ aerogel. Figure 11(b) shows infrared (IR) spectrum of the as-prepared MSQ aerogel. The absorption peaks near 3350, 3470 and 3410 cm^{-1} are assigned as O-H stretches of absorbed water, and a small absorption peak near 1630 cm^{-1} is attributed to the bending vibration of O-H group, which agrees with the results of DTA/TG curves. Small absorption peaks near 2970 cm^{-1} are the results of asymmetric and symmetric stretching vibrations of the C-H group, and two peaks near 1275 and 780 cm^{-1} correspond to the symmetric bending and rocking vibration of Si-CH_3 group. The absorption peaks near 1140, 1040 and 445 cm^{-1} are attributed to O–Si–O bending bond. It indicates that the formation of methylsilsesquioxane with methyl group.

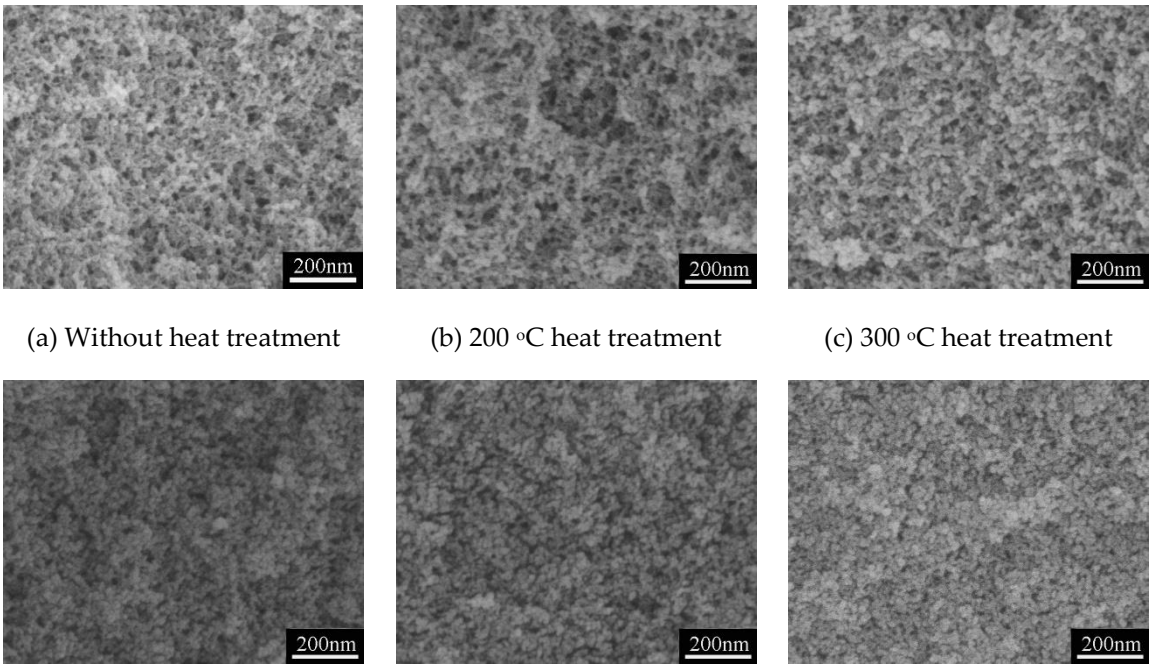

(a) Without heat treatment (b) 200 °C heat treatment (c) 300 °C heat treatment

(d) 400 °C heat treatment (e) 600 °C heat treatment (f) 800 °C heat treatment

Figure 12. SEM images of MSQ aerogels at varied heat treatment temperature.

As we known, thermal stability always has been an important indicator for aerogels, because aerogels are usually applied in a certain condition of temperature, such as heat insulation, catalyst carrier, thermal energy storage and so on. Therefore, heat treatment at 200-800 °C of the typical MSQ aerogel prepared by 500W microwave drying is conducted to investigate the thermal stability of the mesoporous structure as well as the influence of high temperature on the surface area and micropore of the MSQ aerogel. Figure 12 shows SEM images of MSQ aerogels at varied heat treatment temperatures. With the increase of heat treatment temperature, the pore structure of MSQ aerogel gradually decreases, and it becomes more compact, especially at 400, 600 and 800 °C. As observed from the SEM images of the aerogel, collapse of holistic pore structure occurred between 300 and 400 °C, which is corresponding to the temperature of methyl decomposition inferred above in Figure 1a. We infer that it is the exothermic reaction of methyl decomposition resulted in the collapse of holistic pore structure. Figure 13 shows N_2 adsorption–desorption isotherms (a) and BJH mesopore size distributions (b) of MSQ aerogels at varied heat treatment temperatures, and Table 5 shows Pore structure data of the resultant MSQ aerogels. At 200 and 300 °C, the volume absorbed at high relative pressure of aerogel decreases as well as volume absorbed at low relative pressure changed little corresponding to little decrease of specific surface area of aerogel and micropore surface, which

Preprints (www.preprints.org) | NOT PEER-REVIEWED | Posted: 15 January 2019 doi:10.20944/preprints201901.0147.v1

Peer-reviewed version available at Polymers 2019, 11, 375; doi:10.3390/polym11020375

results from shrinkage of mesopores. When heat temperature increases to 400 °C, both volume absorbed at low and high relative pressure and specific surface area of aerogel decreases a lot, indicating the collapse of holistic pore structure by exothermic reaction of methyl decomposition, which is corresponding to SEM images in Figure 12. When the heat treatment is 800 °C, typical MSQ aerogel prepared by 500 W microwave drying still has a specific area of 322 m^2/g and a micropore surface of 210 m^2/g.

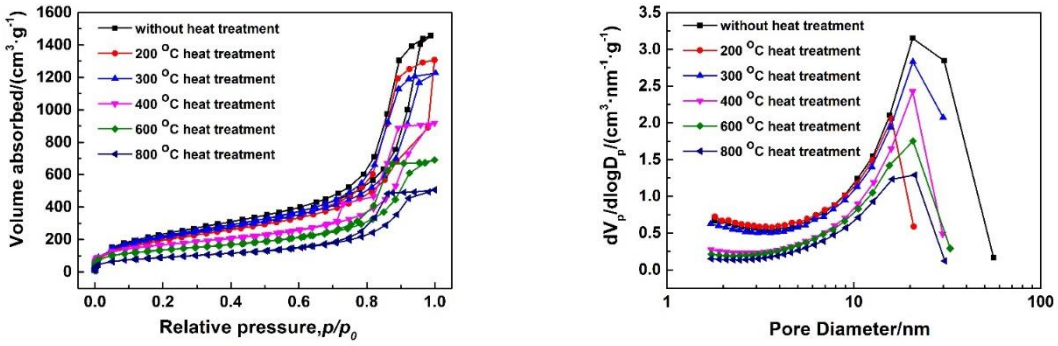

(a) N_2 adsorption–desorption isotherms (b) BJH mesopore size distributions

Figure 13. N_2 adsorption–desorption isotherms (a) and BJH mesopore size distributions (b) of MSQ aerogels at varied heat treatment temperature.

Table 5. Pore structure data of MSQ aerogels at varied heat treatment temperature.

Temperature(°C)	S_p[a](m^2/g)	V_{pore}[b](cc/g)	S_{micro}[c](m^2/g)	V_{micro}[c](cc/g)
Without heat treatment	821	2.2	617	0.3
200	788	2.1	599	0.3
300	738	2.1	545	0.3
400	580	1.5	432	0.2
600	471	1.1	291	0.2
800	322	0.9	210	0.1

[a] Brunauer–Emmett–Teller specific surface area. [b] Pore volume calculated by NLDFT method from the adsorption branch. [c] Micropore surface and volume calculated by the Dubinin-Astakhov method.

2.3. Discussion on microwave drying mechanism of MSQ aerogel

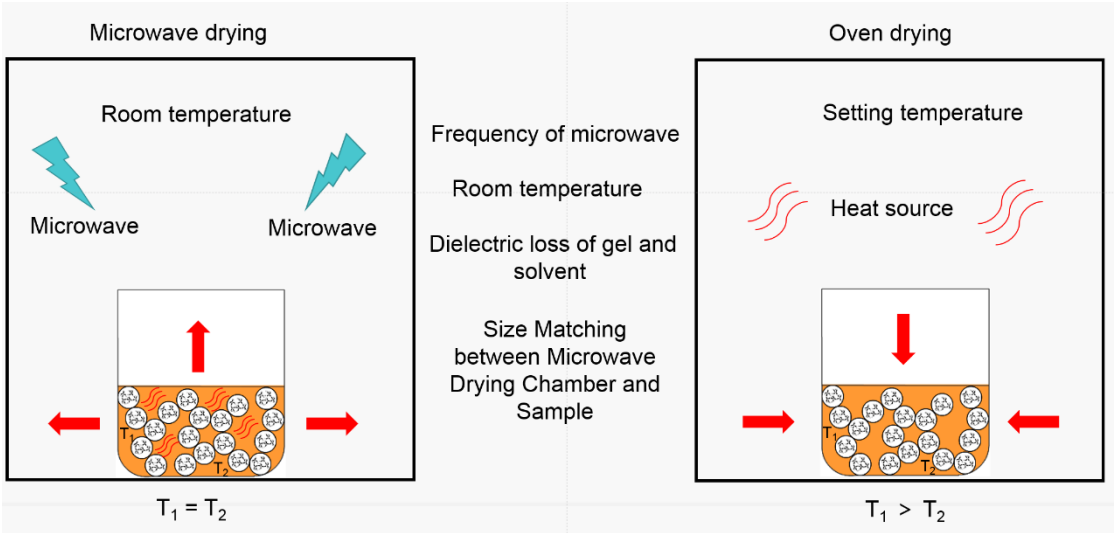

Figure 14. Diagram of microwave drying and oven drying.

Preprints (www.preprints.org) | NOT PEER-REVIEWED | Posted: 15 January 2019 doi:10.20944/preprints201901.0147.v1

Peer-reviewed version available at Polymers 2019, 11, 375; doi:10.3390/polym11020375

Above, we have discussed the influence of microwave power on microstructure of MSQ aerogel in our sol-gel system. However, microwave drying is a new drying method for aerogel and there are still lots of factors can be discussed and researched due to its complicated mechanism. Figure 14 shows the mechanism diagram of microwave drying and oven drying. Different from oven drying, the heat source of microwave drying is evenly distributed within the sample, the reason of which is that microwave heating is achieved by an increase in the overall molecular vibration resulted from interaction between electric dipoles of solvent and alternating electromagnetic field of the microwave. Therefore, the temperature of the different parts of sample are equal during drying. While, the heat source of oven drying is the air in the oven, so there is a heat conduction process from air to the inside of sample, which results in a temperature gradient in the sample. This temperature gradient is one of the main reasons results in the collapse and shrinkage of pore structure during oven drying. Because the heat source of microwave drying is the sample itself, there is still a heat conduction process from sample to air. In our point of view, although this heat conduction process has little influence on the drying effect, it may have a serious impact on efficiency. It is easily to comprehend that when the temperature of air is lower and the size of microwave drying chamber is a lot larger than sample, the frequency of microwave drying should be higher to achieve the drying of MSQ aerogel spending same time. So in order to achieve the quick drying of MSQ aerogel by microwave drying, size matching between microwave drying chamber and sample is essential.

3. Experimental Section

3.1. Materials

Methyltrimethoxysilane (MTMS, Aladdin, shanghai, China, 98%), hydrochloric acid (HCl, Aladdin), hexadecyltrimethylammonium chloride (CTAC, Aladdin, 97%), methanol (Sinopharm Chemical Reagent Co., Ltd., shanghai, China, ≥99.5%), propylene oxide (PO, Sinopharm Chemical Reagent Co., Ltd., shanghai, China, ≥99.5%), 2-propanol (Sinopharm Chemical Reagent Co., Ltd., ≥99.7%), n-heptane (Sinopharm Chemical Reagent Co., Ltd., shanghai, China, ≥98.5%).

3.2. Preparation of MSQ aerogel

Figure 15 shows the reaction scheme and preparation process of MSQ aerogels. Firstly, CTAC, methanol and HCl solution were mixed in a glass tube and then MTMS was added with vigorous stirring and ice-bath for hydrolysis and polymerization of MTMS. After continuously stirring for 30 min, PO was added to the transparent solution (MSQ sol). After stirring for 1~2 min, the resultant solution was allowed to gelate at 40 °C under closed conditions. The gelation time is about 50 min. Then resultant gel was aged over 30 min at the same temperature and firstly solvent exchanged in methanol twice to remove water and CTAC. After methanol solvent replacement, the resultant gel was exchanged in 2-propanol twice and n-heptane twice at 60 °C. Then wet gel with n-heptane was dried by microwave to obtain MSQ aerogel.

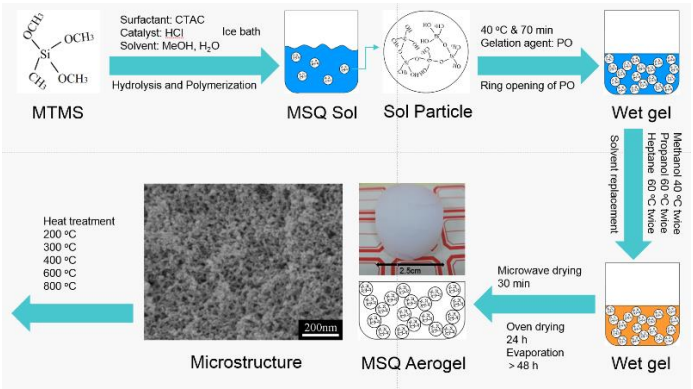

Figure 15. Reaction scheme and preparation process of MSQ aerogels.

3.3. Characterization

Microstructure of MSQ aerogels was observed by scanning electron microscope (SEM: Su8010, Hitachi, Tokyo, Japan) and transmission electron microscope (TEM: JEM-2100, JEOL, Tokyo, Japan). The chemical composition was confirmed by Fourier transform infrared spectroscopy (FT-IR, Nicolet 6700, ThermoFisher Scientific, Waltham, MA, USA), differential thermal analysis (DTA, Q200, TA, New Castle, DE, USA) and thermogravimetry (TG, TA-Q500, TA, New Castle, DE, USA). Pore structure of MSQ aerogels was characterized by using an N_2 adsorption–desorption apparatus (BET, ASAP2020HD88, Micromeritics Instruments Corporation, Norcross, GA, USA), and the samples were degassed at 120 °C under vacuum before each N_2 adsorption–desorption measurement. The BJH method was applied to the adsorption branch to derive mesopore size distributions.

4. Conclusions

Methylsilsesquioxane aerogels with uniform mesopores have been facilely prepared via a sol–gel process by microwave drying. The influences of gelation agent, catalyst, solvent and microwave power on pore structure were investigated in detail to achieve controllable preparation of MSQ aerogels, and the thermal stability of MSQ aerogels are also analyzed. MSQ aerogel by 500 W microwave drying possessed a specific surface area up to 821 m^2/g and a mesopore size of 20 nm. After heat treatment of 800 °C, MSQ aerogel prepared by 500W microwave drying still had a specific area of 322 m^2/g and a micropore surface of 210 m^2/g. To pave the way for the follow-up researches on microwave drying, mechanism of microwave drying was discussed in detail and size matching between microwave drying chamber and sample was considered essential for drying efficiency.

Acknowledgments: This work is supported by the High Science & Technique Brainstorm Project of Zhejiang Province of China (No. 2017C01002), the National Natural Science Foundation of China (21875217 and 51372225) and Industry-University-Research Collaboration Project of Jiangsu Province (FZ20180405).

Author Contributions: Xingzhong Guo and Jiaqi Shan conceived and designed the experiments; Jiaqi Shan performed the experiments; Xingzhong Guo and Jiaqi Shan analyzed the data; Wei Lei, Ronghua Ding and Zhang Yun contributed reagents/materials/analysis tools; Xingzhong Guo and Jiaqi Shan wrote the paper.

Conflicts of Interest: The authors declare no conflict of interest.

References

1. Dorcheh, A.S.; Abbasi, M.H. Silica aerogel; synthesis, properties and characterization. *J Mater Process Tech* **2008**, *199*, 10-26, doi: 10.1016/j.jmatprotec.2007.10.060.
2. Hüsing, N.; Schubert, U. Aerogels-Airy Materials: Chemistry, Structure, and Properties. *Angew Chem Int Edit* **2010**, *37*, 22-45, doi: 10.1002/(SICI)1521-3773(19980202)37:1/2<22::AID-ANIE22>3.0.CO;2-I.
3. Hrubesh, L.W. Aerogels: the world's lightest solids. ***Chem Ind-London*** **1990**, *24*, 824-827.
4. Aegerter, M.; Leventis, N.; Koebel, M.M. *Aerogels handbook*; Springer Science & Business Media: Berlin, German, 2011.
5. Chen, M.M.; Zhang, L.; Li, J.H.; Li, J.Y.; Li, Q.N.; Zhang, L. The extraction of uranium using graphene aerogel loading organic solution. *Talanta* **2017**, *166* 284-291, doi: 10.1016/j.talanta.2017.01.070.
6. Wang, L.J.; Wang, Y.S.; Wang, X.X.; Feng, X.L.; Ye, X.; Fu, J. Small-Sized Mg-Al LDH Nanosheets Supported on Silica Aerogel with Large Pore Channels: Textural Properties and Basic Catalytic Performance after Activation. *Nanomaterials-Basel* **2018**, *8*, 113, doi: 10.3390/nano8020113.
7. Alnaief, M.; Antonyuk, S.; Hentzschel, C.M.; Leopold, C.S.; Heinrich, S.; Smirnova, I. A novel process for coating of silica aerogel microspheres for controlled drug release applications. *Micropor Mesopor Mat* **2012**, *160*, 167-173, doi: 10.1016/j.micromeso.2012.02.009.
8. Murphy, E.F.; Schmid, L.; Burgi, T.; Maciejewski, M.; Baiker, A.; Gunther, D.; Schneider, M. Nondestructive sol-gel immobilization of metal (salen) catalysts in silica aerogels and xerogels. *Chem Mater* **2001**, *13*, 1296-1304, doi: 10.1021/cm001187w.
9. Li, C.H.; Jiang, S.C.; Yao, Z.P.; Sheng, S.; Jiang, X.J.; Zhou, B.; Du, A. Research on Heat Transfer Characteristics of Nano-porous Silica Aerogel Material and its Application on Mars surface Mission. *Adv Mater Res* **2014**, *924*, 329-335, doi: 10.4028/www.scientific.net/AMR.924.329.

10. He, Y.L.; Xie, T. Advances of thermal conductivity models of nanoscale silica aerogel insulation material. *Appl Therm Eng* **2015**, *81*, 28-50, doi: 10.1016/j.applthermaleng.2015.02.013.
11. Jiang, X.Q. ; Wang, D.; Yao, J.X.; Mao, D.; Xing, C.J.; Lai, X.Y. Preparation of SiO_2 Aerogels Heat Insulation Composites Reinforced by Aramid Fiber. *Rare Metal Mat eng* **2009**, *38*, 354-357.
12. Kaya, G.G.; Yilmaz, E.; Deveci, H. Sustainable nanocomposites of epoxy and silica xerogel synthesized from corn stalk ash: Enhanced thermal and acoustic insulation performance. *Compos Part B-Eng* 2018, *150*, 1-6, doi: 10.1016/j.compositesb.2018.05.039.
13. Cotana, F.; Pisello, A.L.; Moretti, E.; Buratti, C. Multipurpose characterization of glazing systems with silica aerogel: In-field experimental analysis of thermal-energy, lighting and acoustic performance. *Build Environ* **2014**, *81*, 92-102, doi: 10.1016/j.buildenv.2014.06.014.
14. Eskandari, N.; Motahari, S.; Atoufi, Z.; Motlagh, G.H.; Najafi, M. Thermal, mechanical, and acoustic properties of silica-aerogel/UPVC composites. *J Appl Polym Sci* **2017**, *134*, 44685, doi: 10.1002/app.44685.
15. Tabata, M.; Adachi, I.; Kawai, H.; Kubo, M.; Sato, T. Recent progress in silica aerogel Cherenkov radiator. *Phys Procedia* **2012**, *37*, 642-649, doi: 10.1016/j.phpro.2012.02.410.
16. Shao, Z.D.; Cheng, X.; Zheng, Y.M. Facile co-precursor sol-gel synthesis of a novel amine-modified silica aerogel for high efficiency carbon dioxide capture. *J Colloid Interf Sci* **2018**, *530*, 412-423, doi: 10.1016/j.jcis.2018.06.094.
17. Firoozmandan, M.; Moghaddas, J.; Yasrebi, N. Performance of water glass-based silica aerogel for adsorption of phenol from aqueous solution. *J Sol-Gel Sci Techn* **2016**, *79*, 67-75, doi: 10.1007/s10971-016-4007-2.
18. Faghihian, H.; Nourmoradi, H.; Shokouhi, M. Removal of copper (II) and nickel (II) from aqueous media using silica aerogel modified with amino propyl triethoxysilane as an adsorbent: equilibrium, kinetic, and isotherms study. *Desalin Water Treat* **2014**, *52*, 305-313, doi: 10.1080/19443994.2013.785367.
19. Zhang, C.Z.; Dai, C.; Zhang, H.Q.; Peng, S.T.; Wei, X.; Hu, Y.D. Regeneration of mesoporous silica aerogel for hydrocarbon adsorption and recovery. *Mar Pollut Bull* **2017**, *122*, 129-138, doi: 10.1016/j.marpolbul.2017.06.036.
20. Huang, X.Y.; Liu, Z.P.; Xia, W.; Zou, R.Q.; Han, Ray P.S. Alkylated phase change composites for thermal energy storage based on surface-modified silica aerogels. *J mater chem A* **2015**, *3*, 1935-1940, doi: 10.1039/c4ta06735e.
21. Kistler, S.S. Coherent expanded aerogels and jellies. *Nature* **1931**, *127*, 741, doi: 10.1038/127741a0.
22. Kanamori, K.; Aizawa, M.; Nakanishi, K.; Handa, T. Elastic organic–inorganic hybrid aerogels and xerogels. *J Sol-Gel Sci Technol* **2008**, *48*, 172–181, doi:10.1007/s10971-008-1756-6.
23. Hayase, G.; Kanamori, K.; Fukuchi, M.; Kaji, H.; Nakanishi, K. Facile synthesis of marshmallow-like macroporous gels usable under harsh conditions for the separation of oil and water. *Angew Chem* **2013**, *52*, 1986–1989, doi:10.1002/anie.201207969.
24. Rao, A.V.; Kulkami, M.M.; Amalnerkar, D.P.; Seth, T. Superhydrophobic silica aerogels based on methyltrimethoxysilane precursor. *J Non-Cryst Solids* **2003**, *330*, 187–195, doi:10.1016/j.jnoncrysol.2003.08.048.
25. Guo, X.Z.; Li, W.Y.; Yang, H.; Kanamori, K.; Zhu, Y.; Nakanishi, K. Pore structure control of macroporous methylsilsesquioxane monoliths prepared by in situ two-step processing. *J Porous Mater* **2013**, *20*, 1477–1483, doi:10.1007/s10934-013-9733-z.
26. Guo, X.Z.; Li, W.Y.; Yang, H.; Kanamori, K.; Zhu, Y.; Nakanishi, K. Gelation behavior and phase separation of macroporous methylsilsesquioxane monoliths prepared by in situ two-step processing. *J Sol-Gel Sci Technol* **2013**, *67*, 406–413, doi:10.1007/s10971-013-3094-6.
27. He, S.; Li, Z.; Shi, X.J.; Yang, H.; Gong, L.L.; Cheng, X.D. Rapid synthesis of sodium silicate based hydrophobic silica aerogel granules with large surface area. *Adv Powder Technol* **2015**, *26*, 537-541, doi: 10.1016/j.apt.2015.01.002.
28. Hayase, G.; Kanamori, K.; Maeno, A.; Kaji, H.; Nakanishi, K. Dynamic spring-back behavior in evaporative drying of polymethylsilsesquioxane monolithic gels for low-density transparent thermal superinsulators. *J Non-Cryst Solids* **2016**, *434*, 115-119, doi: 10.1016/j.jnoncrysol.2015.12.016.
29. Guo, X.Z.; Li, W.Y.; Zhu, Y.; Nakanishi, K.; Kanamori, K. Macroporous SiO_2 monoliths prepared via sol-gel process accompanied by phase separation. *Acta Phys.-Chim. Sin.* **2013**, *29*, 646–652, doi:10.3866/PKU.WHXB201212252.
30. Yang, H.; Ding, Z.S.; Jiang, Z.H.; Xu, X.P. Sol-gel process kinetics for $Si(OEt)_4$. *J Non-Cryst Solids* **1989**, 112, 449-453, doi.org/10.1016/0022-3093(89)90571-1.

31. Nakanishi, K. Sol-gel process of oxides accompanied by phase separation. *B Chem Soc Jpn* **2006**, *79*, 673-691, doi: 10.1246/bcsj.79.673.
32. Nakanishi, K. Pore Structure Control of Silica Gels Based on Phase Separation. *J Porous Mat* **1997**, 4, 67-112, doi: 10.1023/a:1009627216939.

Sample Availability: Samples of the MSQ aerogels are available from the authors.